Nucleic Acids Research Advance Access published July 21, 2015

Nucleic Acids Research, 2015 **1**
doi: 10.1093/nar/gkv723

The yeast genome undergoes significant topological reorganization in quiescence

Mark T. Rutledge[1,2], Mariano Russo[1], Jon-Matthew Belton[3], Job Dekker[3] and James R. Broach[1,*]

[1]Department of Biochemistry and Molecular Biology, Penn State College of Medicine, Hershey, PA 17033, USA, [2]Department of Molecular Biology, Princeton University, Princeton, NJ 08544, USA and [3]Program in Systems Biology, University of Massachusetts Medical School, Worcester, MA 01605, USA

Received February 05, 2015; Revised July 02, 2015; Accepted July 06, 2015

ABSTRACT

We have examined the three-dimensional organization of the yeast genome during quiescence by a chromosome capture technique as a means of understanding how genome organization changes during development. For exponentially growing cells we observe high levels of inter-centromeric interaction but otherwise a predominance of intrachromosomal interactions over interchromosomal interactions, consistent with aggregation of centromeres at the spindle pole body and compartmentalization of individual chromosomes within the nucleoplasm. Three major changes occur in the organization of the quiescent cell genome. First, intrachromosomal associations increase at longer distances in quiescence as compared to growing cells. This suggests that chromosomes undergo condensation in quiescence, which we confirmed by microscopy by measurement of the intrachromosomal distances between two sites on one chromosome. This compaction in quiescence requires the condensin complex. Second, inter-centromeric interactions decrease, consistent with prior data indicating that centromeres disperse along an array of microtubules during quiescence. Third, inter-telomeric interactions significantly increase in quiescence, an observation also confirmed by direct measurement. Thus, survival during quiescence is associated with substantial topological reorganization of the genome.

INTRODUCTION

The organization of the genome within the nuclei of cells of the same type is remarkably consistent from cell to cell, promoting and reflecting genome function. In all actively growing cells rDNA is sequestered in the nucleolus, a distinct compartment organized around the synthesis of rRNA for subsequent assembly into ribosomes. In nuclei of metazoan cells, individual chromosomes inhabit distinct domains in a stereotypic fashion across most cells (1,2). Whether such three-dimensional (3D) organization provides local addresses to facilitate gene expression or other functions remains to be resolved. In interphase mammalian cell nuclei, regions of heterochromatin lie adjacent to the nuclear membrane and around nucleoli. This structure undergoes dramatic reorganization in senescent cells, with certain heterochromatic regions migrating from the periphery to the interior and while other domains move from the interior to the periphery (3). The functional consequences of this reorganization are unclear. Nonetheless, these results suggest that interrogating the organization of the genome in cells under different developmental conditions may provide information on the function of different regions of the genome in those conditions and define the interplay of genome structure and function during developmental transitions.

The yeast *Saccharomyces cerevisiae* provides a facile system for correlating genome organization and function as that organization is modified during developmental progression (4). Several functional constraints drive the 3D structure of the yeast genome within the nucleus of actively growing cells. A primary organizing principle is segregation of chromosomes at mitosis. As a consequence of the closed mitosis and the retention of the nuclear membrane, yeast centromeres remain attached to a mitotic spindle throughout the cell cycle, residing near the spindle pole body and thus in close proximity to one another at all times (5–7). Furthermore, chromosome arms, which lag behind the centromeres during mitosis and anaphase, retain that wishbone-like, or Rabl, configuration throughout the cell cycle with the trailing telomeres remaining associated with the nuclear membrane and often clustered near each other (8,9). This geometric structure results in close physical association of telomeres on chromosome arms of equal length (10,11). The second organizing principle, as noted above, is the sequestration of rDNA within the nucleolus. In addi-

*To whom correspondence should be addressed. Tel: +1 717 531 8586; Fax: +1 717 531 7072; Email: jbroach@hmc.psu.edu

tion, tRNA genes have been reported to cluster with each other and near the periphery of the nucleolus, perhaps reflecting both an aggregation of Polymerase III complexes in the nucleus and an association of the transcription complex with the rDNA organization (12–14). Finally, some evidence suggests that DNA replication takes place on discrete loci within the nucleus, where the replication machinery remains stationary and DNA strands migrate through during replication (15–18). Thus, the yeast genome exhibits extensive 3D organization during exponential growth.

We have examined the 3D organization of the genome during quiescence as a means of understanding how genome organization changes under significant transcriptional and structural reprogramming during development. In yeast, starvation for any of several essential nutrients elicits exit from the mitotic cycle and entry into a poorly defined quiescent state, designated as G0 (19,20). The only unequivocal property of cells in quiescence is the ability to retain viability over extended time and to return to mitotic growth when the limiting nutrient is restored (21). Many other properties attributed to quiescent cells, such as heat shock resistance, increased cell wall thickness, resistance to oxidative damage, etc., have been shown to be simply extreme extensions of properties acquired as cells grow more slowly (21,22). Thus, unequivocal markers of quiescent cells remain elusive and the critical properties that allow cells to retain viability over extend time remain poorly defined.

Most studies of quiescence in yeast have focused on stationary cells—those cells grown in rich media following depletion of glucose and subsequent depletion of the resultant ethanol produced by fermentation of the glucose (19). This process yields a mixture of viable and nonviable cells with quite distinct physiological and metabolic properties (23). We have found that depletion of different nutrients—glucose, nitrogen, phosphate or sulfur—from cells growing in rich media all elicit a quiescent state, as judged by the ability of cells to retain viability for extended time and to resume growth following re-addition of the missing nutrient (21). Even though cells starved for different nutrients exhibit different transcriptional, metabolic and proteomic responses depending on the limited nutrient, the response of cells to any one particular starvation is uniform, yielding a single population of fully viable cells.

All quiescent cells appear to exhibit one characteristic that is independent of the starvation regimen used to elicit quiescence—namely, genome organization. Many years ago, Piñon and colleagues demonstrated that chromatin of starved cells sedimented as a distinct structure in sucrose gradients but with a different velocity than did chromatin of either G1 or G2 phase cells (24). The sedimentation rate of chromatin from quiescent cells was identical whether cells were induced into quiescence by starvation for glucose, nitrogen or sulfur. Thus, the investigators proposed that quiescence, regardless of its etiology, was associated with a specific organizational alteration of the genome. Consistent with this hypothesis, the DNaseI sensitivity of chromatin from quiescent cells is significantly less than that from growing cells (25). We have examined the nature of that altered organization by applying a global chromosome conformation capture technique, referred to as Hi-C, that identifies to what regions of the genome each site within the genome is in proximity. This analysis confirms that the organization of the genome in quiescent cells is distinct from that in growing cells. Moreover, the results from this study define the specific nature of that reorganization and are consistent with recent observations regarding the reorganization of cellular structures within yeast cells induced into quiescence (26). Finally, these observations provide insight into the nature of quiescence and the ability of such cells to survive extended periods of starvation.

MATERIALS AND METHODS

Strain construction

All *S. cerevisiae* strains used in this study are listed in Table 1. They were derived from strains of either the W303 or S288C backgrounds and were created using standard yeast methods (27). Strain Y4158, derived from strain Y3904 by sporulation, was transformed with a polymerase chain reaction (PCR) fragment encoding sequences with homology to the *CAN1* locus flanking a KanR cassette preceded by a GFP-*Lac*I fusion gene driven by the *S. cerevisiae HIS3* promoter and a *Tet*R-mCherry fusion gene driven by the *S. cerevisiae URA3* promoter to generate strain Y4159. Insertion of *Lac*O and *Tet*R arrays at specific loci was accomplished as described previously (28) by transforming strain Y2963 with plasmids pPJS181, pPJS225 and pPJS274 (Table 2) to generate strain Y4160, Y4161 and Y4162, respectively. All integrations were verified by sequencing PCR products from the insertion site. The resulting strains were mated with Y4159 to generate diploids used for imaging. The strain Y4166 was constructed by mating strains Y4159 and Y2961 to generate a strain used to visualize the spatial distances between two loci on chromosome IX. The KanMX cassette of strain Y4159 was then replaced with LEU2 in order to allow for G418 resistance to be used in making mutants of this strain. This strain and Y2961 were each transformed with PCR fragments encoding temperature sensitive alleles for either *smc1–2*, to produce strains Y4167 and Y4168, or *smc2–8*, to produce strains Y4169 and Y4170, both tagged by a KanMX cassette for selection. Strains Y4167 and Y4168 were mated to produce the homozygous *smc1–2* diploid Y4171, and Y4169 and Y4170 were mated to produce the homozygous *smc2–8* diploid Y4172. To visualize telomeric foci strain Y4173 containing Rap1-GFP and Hta1-mCherry alleles (29) was mated to Y3358 to produce a prototrophic diploid Y4174. The larger nuclear volume in diploid cells provides for higher resolution in single cell imaging (28).

Microscopy and image processing

For comparison of exponential growth and 1-day glucose-starved quiescence, single colonies of strains Y4163, Y4164, Y4165 and Y4166 were each grown overnight at 30°C and inoculated into fresh 3 ml SD cultures (27) and grown for 7–8 h to 1. x 10^7 cells per ml. Cells were concentrated by centrifugation and 10 μl of cells were placed on a 24 mm x 60 mm glass cover slip and covered by an agar pad approximately 15 mm x 15 mm x 5 mm. The rest of the culture was pelleted by quick centrifugation, washed twice with SD lacking glucose, resuspended in 2.5 ml SD lacking glucose

Table 1. Yeast strains used in this study

Name	MT	Genotype	Background	Reference
Y3358	a	*HIS3 LEU2 TRP1 URA3*	W303	(21)
Y3904	a/α	*his3–11,15/HIS3 leu2–3,112/LEU3 trp1–1/TRP1 ura3–1/URA3 can1–100/can1–100*	W303	This study
Y4158	α	*HIS3 leu2–3,112 TRP1 ura3–1 can1–100*	W303	This study
Y4159	α	*HIS3 leu2–3,112 TRP1 ura3–1 can1*::P_{HIS3}-GFP-*Lac*I:P_{URA3}-*Tet*R-mCherry:KanMX6	W303	This study
Y2963	a	*leu2 ura3 trp1 his3* chrIX-421kb::*Tet*O_{112}:*URA3 can1–100*	S288C	(28)
Y4160	a	*leu2 ura3 trp1 his3* chrIX-421kb::*Tet*O_{112}:*URA3* chrIII-297k:*Lac*O_{256}:*LEU2*	S288C	This study
Y4161	a	*leu2 ura3 trp1 his3* chrIX-421kb::*Tet*O_{112}:*URA3* chrIII-17k:*Lac*O_{256}:*LEU2*	S288C	This study
Y4162	a	*leu2 ura3 trp1 his3* chrIX-421kb::*Tet*O_{112}:*URA3* chrIX-16k:*Lac*O_{256}:*LEU2*	S288C	This study
Y4163	a/α	*leu2/leu2 ura3/ura3 trp1/TRP1 his3/HIS3 can1/can1*::P_{HIS3}-GFP-*Lac*I:P_{URA3}-*Tet*R-mCherry:KanMX6 chrIX-421kb::*Tet*O_{112}:*URA3*/chrIX chrIII-297kb:*Lac*O_{256}:*LEU2*/chrIII	S288C /W303	This study
Y4164	a/α	*leu2/leu2 ura3/ura3 trp1/TRP1 his3/HIS3 can1–100/can1*::P_{HIS3}-GFP-*Lac*I:P_{URA3}-*Tet*R-mCherry:KanMX6 chrIX-421kb::*Tet*O_{112}:*URA3*/chrIX chrIII-17kb:*Lac*O_{256}:*LEU2*/chrIII	S288C /W303	This study
Y4165	a/α	*leu2/leu2 ura3/ura3 trp1/TRP1 his3/HIS3 can1–100/can1*::P_{HIS3}-GFP-*Lac*I:P_{URA3}-*Tet*R-mCherry:KanMX6 chrIX-421kb::*Tet*O_{112}:*URA3*/chrIX chrIX-16kb:*Lac*O_{256}:*LEU2*/chrIX	S288C /W303	This study
Y2961	a	*leu2 ura3 trp1 his3 can1* chrIX-225kb::*Tet*O_{112}:*URA3* chrIX-106kb:*Lac*O_{256}:*LEU2*	S288C	(28)
Y4166	a/α	*leu2/leu2 ura3/ura3 trp1/TRP1 his3/HIS3 can1/can1*::P_{HIS3}-GFP-*Lac*I:P_{URA3}-*Tet*R-mCherry:KanMX6 chrIX-225kb::*Tet*O_{112}:*URA3*/chrIX chrIX-106kb:*Lac*O_{256}:*LEU2*/chrIX	S288C /W303	This study
Y4167	a	*leu2 ura3 trp1 his3 can1* chrIX-225kb::*Tet*O_{112}:*URA3* chrIX-106kb:*Lac*O_{256}:*LEU2 smc1–2:KanMX*	S288C	This study
Y4168	α	*HIS3 leu2–3,112 TRP1 ura3–1 can1::*P_{HIS3}*-GFP-LacI:*P_{URA3}*-TetR-mCherry:LEU2 smc1–2:KanMX*	W303	This study
Y4169	a	*leu2 ura3 trp1 his3 can1 chrIX-225kb::TetO*$_{112}$*:URA3 chrIX-106kb:LacO*$_{256}$*:LEU2 smc2–8:KanMX*	S288C	This study
Y4170	α	*HIS3 leu2–3,112 TRP1 ura3–1 can1::*P_{HIS3}*-GFP-LacI:*P_{URA3}*-TetR-mCherry:LEU2 smc2–8:KanMX*	W303	This study
Y4171	a/α	*leu2/leu2 ura3/ura3 trp1/TRP1 his3/HIS3 can1/can1::*P_{HIS3}*-GFP-LacI:*P_{URA3}*-TetR-mCherry:LEU2 chrIX-225kb::TetO*$_{112}$*:URA3/chrIX chrIX-106kb:LacO*$_{256}$*:LEU2/chrIX smc1–2:KanMX/smc1–2:KanMX*	S288C /W303	This study
Y4172	a/α	*leu2/leu2 ura3/ura3 trp1/TRP1 his3/HIS3 can1/can1::*P_{HIS3}*-GFP-LacI:*P_{URA3}*-TetR-mCherry:LEU2 chrIX-225kb::TetO*$_{112}$*:URA3/chrIX chrIX-106kb:LacO*$_{256}$*:LEU2/chrIX smc2–8:KanMX/smc2–8:KanMX*	S288C /W303	This study
Y4173	a	*ura3–1 leu2,3–112 his3–1 ade2–1 can1–100 Δbar1 HTA1-mCherry::URA3 trp1–1::RAP1-GFP::TRP1*	W303	(29)
Y4174	*a*/α	*his3–1/HIS3 leu2,3–112/leu2–3,112 trp1–1::RAP1-GFP::TRP1/TRP1 ura3–1/ura3–1 can1–100/can1–100 Δbar1/BAR1 HTA1-mCherry::URA3/HTA1 ade2–1/ADE2*	W303/W303	This study

Table 2. Plasmids used in this study

Name	Yeast genes	Bacterial genes	Background	Reference
pPJS181	chrIII-297k:LacO$_{256}$:*LEU2*	bla	STBL2	This study
pPJS225	chrIII-17k:LacO$_{256}$:*LEU2*	bla	STBL2	This study
pPJS274	chrIX-16k:LacO$_{256}$:*LEU2*	bla	STBL2	This study

and incubated at 30°C for 24 h before preparing another aliquot of cells as above. The same procedure was used to compare exponential growth to 1-day nitrogen-starved quiescence except that cultures were grown in nitrogen-limiting medium before being pelleted, washed and resuspended in SD lacking nitrogen (see (21)). Telomeric foci were prepared for imaging similarly using strain Y4174. The temperature sensitive experiments using strains Y4171 and Y4172 were performed in a similar manner except that they were grown at 23°C and then shifted to 37°C for 3 h with imaging being done for each of the two time points. Slides were imaged immediately after preparation on a DeltaVision Elite deconvolution microscope (Applied Precision) fitted with a 100x objective (1.4 numerical aperture) at 22°C. The images were taken with a Photometrics CoolSNAP HQ2 charge-coupled device camera. Stacks spaced 0.25 um totaling 5–6 um were acquired, and the images were deconvolved using the Applied Precision SoftWorx built-in deconvolution software. The deconvolved images were analyzed in ImageJ (30) with the Bio-Formats plugin (31) using a custom script that prompts the user to mark the nucleus for each cell containing a single, clearly visible spot for both the red

and green channels and then computes the 3D distance between the brightest red and green pixels within the marked area. The resultant data were statistically analyzed using the Kolmogorov–Smirnov or Mann-Whitney U-tests to assess the difference in the distributions of spots. The results were visualized in R using a custom script making use of the following libraries: ggplot2, RColorBrewer, plyr, reshape2. Telomeric foci were found using the 'Find Maxima' feature in ImageJ using a threshold value chosen to very conservatively minimize the possibility for spurious spot detection.

Hi-C

Two 400 ml cultures of Y3358 in SD were inoculated from a fresh overnight culture and grown for 11–12 h to an optical density at A600 of 0.8–1.0. One culture was immediately fixed with formaldehyde (Sigma F8775–25ML) at a final concentration of 3% for 20 min shaking at 25°C before being quenched with 2.5 M glycine for 5 min shaking at 25°C. The culture was then harvested by centrifugation and washed twice with 10 ml dH_2O and then resuspended in 3 ml of 1X NEBuffer 2 (New England Biolabs B7002S). A small aliquot of cell suspension was kept to subsequently determine the concentration of cells. The cell suspension was dripped by pipette into a tube containing liquid nitrogen to flash freeze the cells as small droplets. The frozen cell droplets were cryogenically lysed using a Retsch Cryomill (Retsch 0.749.0001) operating at 20 Hz for 20 min. The frozen and ground cell suspension was gently thawed on ice before being spun down and washed twice with 10 ml 1X NEBuffer 2. The resulting suspension was diluted to an optical density at A600 of 5.0 and 6 ml of the suspension was used for subsequent analysis. The second culture was filtered, washed twice with SD lacking glucose, resuspended in 400 ml of SD lacking glucose, incubated at 30°C in a shaking incubator for 24 h and then processed as above.

Hi-C was performed essentially as described (32). The final libraries of paired fragments were sequenced on an Illumina HiSeq 2500 using the TruSeq PE Cluster Kit v3 and the TruSeq SBS Kit v3 (Illumina PE-401–3001 and FC-401–3001, respectively) to generate 100 base paired-end reads. One half of a lane was used for each library, generating about 100 million mate pairs of sequencing events per library. The mate pairs of individual sequencing events were aligned to the W303 assembly of the yeast genome (33) using the Bowtie software (34) to assign each end of the DNA fragment a single position within the W303 genome. After removal of any duplicate sequencing events or events whose mate-pairs map to the same fragment (self circles and unligated DNA ends that were missed during the biotin removal step) the mapped interactions produced around 40 million unique valid pair interactions per sample that were then iteratively corrected as previously described (35) (Table 3). The iteratively-corrected interaction data from each sample were normalized to the total number of reads within the sample in order to observe relative differences in interaction frequency between multiple samples. All data analysis of the normalized data was performed in R.

Table 3. Hi-C library statistics

Statistic	Exponential growth	Quiescence
Total sequencing reads	111,626,167	84,063,556
Reads mapped	75,343,368	58,770,429
Unique valid pairs	39,109,904	34,870,633
Self circles	8,554,309	2,314,772
Dangling ends	11,614,721	11,613,712
PCR duplicates	8,933,614	1,335,355

RESULTS

To investigate how the 3D conformation of the DNA of yeast cells changes with changing environmental conditions, we performed Hi-C experiments on yeast cells in exponential growth on glucose-containing medium and on yeast cells in quiescence induced by glucose starvation. Glucose starvation was accomplished by filtration of prototrophic cultures growing in synthetic minimal glucose medium followed by washing and resuspension in prewarmed synthetic minimal medium lacking glucose. This starvation procedure elicits substantial immediate changes in the transcriptome, metabolome and proteome of cells but these profiles stabilize after one day and remain constant for many days thereafter, indicating that cells enter a stable state within one day (21). Moreover, almost all cells maintain viability under this condition and retain the ability to reenter the cell division cycle once reintroduced into glucose medium, suggesting that this stable state is a form of quiescence (21). Physiological, transcriptional and proteomic studies document that this state is distinct from that of cells that enter quiescence through the exhaustion of external carbon during the progression to stationary phase and the two growth trajectories mimic two different natural phenomena: immediate starvation following rapid transition to a nutrient depleted environment versus continuously adaptive starvation in progressively limiting fermentation conditions. We chose the comparison of exponential growth to immediate glucose starvation because all cells respond uniformly to that event and because it mimics an extreme, immediate environmental change while limiting the changing environmental elements to only a single variable: whether or not the cells have access to an external carbon source.

Hi-C captures the physical contacts between genomic loci in a manner that allows the interrogation of all pairwise interactions of unique sequences within the genome (36). Briefly, this is accomplished by formaldehyde fixation to preserve chromatin contacts, restriction enzyme digestion, intramolecular ligation, isolation of ligated fragments and paired-end sequencing of the ligation products to determine to where in the genome each side uniquely maps (Figure 1A). After filtering for true interactions the sequencing data are corrected for experimental biases and normalized to the total number of reads within the sample before being partitioned into genomic bins sized 10 kb pairs (35). This bin size is conservatively larger than the average distance between two genomic restriction sites used to generate the sequenced fragments. The resulting data are an all-by-all two-dimensional matrix of sequencing reads where each column and each row correspond to a specific genomic bin and the

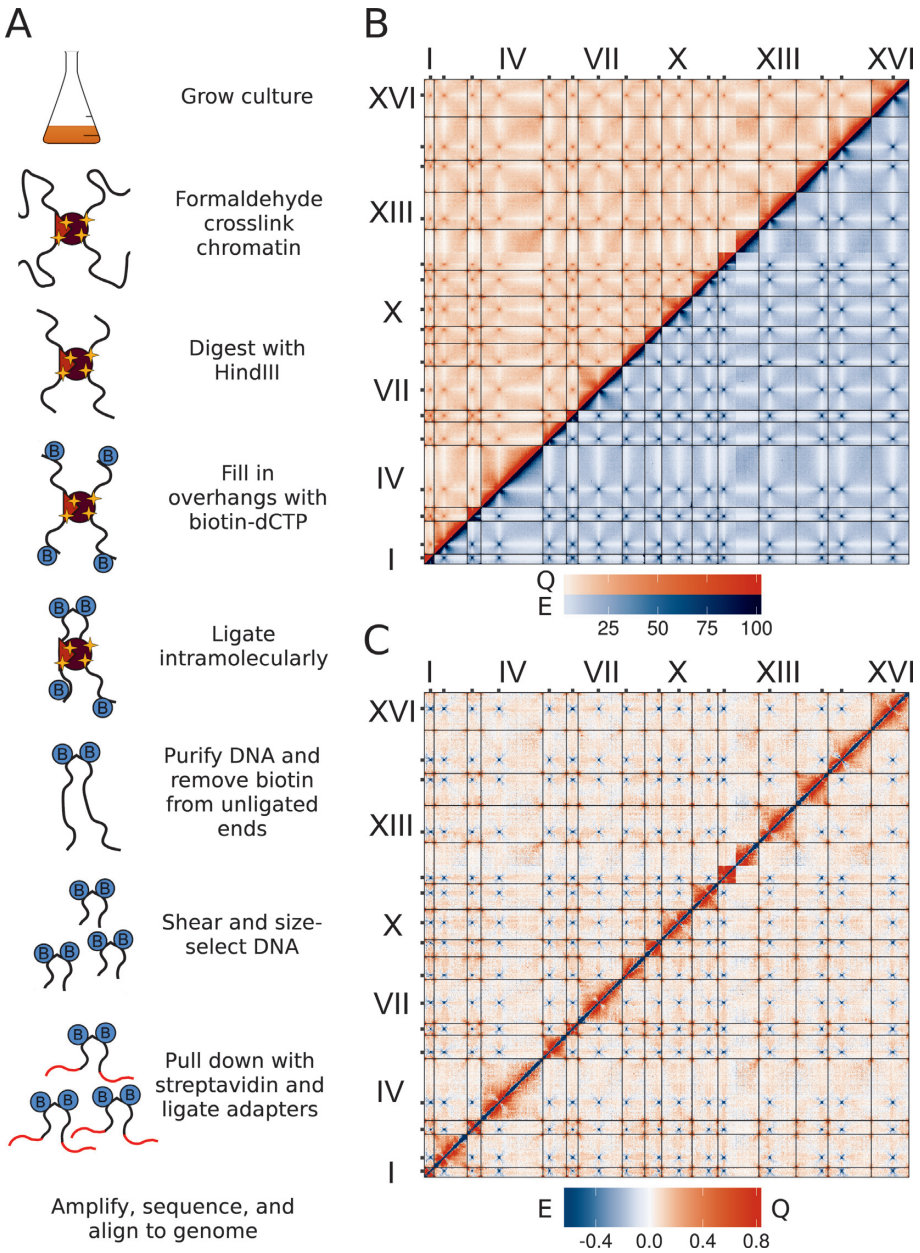

Figure 1. The yeast genome undergoes large scale reorganization in quiescence. (**A**) A graphic depiction of the experimental Hi-C method. (**B**) Interaction frequency data matrix for each individual growth condition: exponential growth in blue below the diagonal, quiescence in orange above the diagonal. Data points represent 10 kb-pair genomic bins for any two given genomic loci for which sequencing reads from true interactions were obtained. Chromosomes are labeled periodically along the axes and are visually separated by black bars. Centromeric regions are marked with gray squares along the axes. Data values for each bin are normalized to the total the number of sequencing reads within the sample and are shown as percentages of the highest value for the sample. To better visually depict a broad range of interaction levels, data values falling outside of the 3rd to 97th percentiles of the total range are set equal to the lowest or highest values within this truncated range, respectively. (**C**) Differential interaction frequency data matrix comparing Hi-C data from the two growth states. Data values from (B) are represented here as quiescent signal minus exponential growth signal and are centered around no change between growth states by Z-scoring the differential data set. Blue (negative) and orange (positive) values represent genomic interactions that occur more frequently relative to other intra-sample genomic interactions in exponential growth and quiescence, respectively. Similar to (B) the data values were modified to fit within a range spanning the 2nd to 98th percentiles of the total range for ease of visualization.

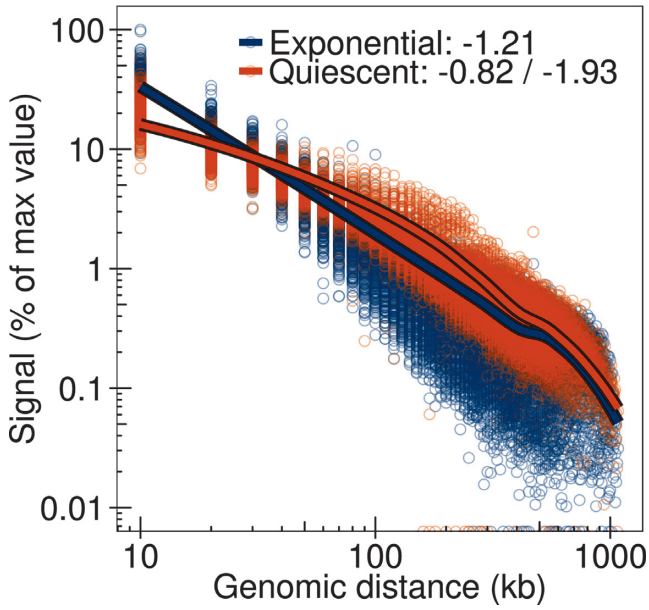

Figure 2. Polymer scaling of chromosomes shows differences in compaction between the two growth states. Interaction frequencies for all genomic loci are plotted against distance between the interacting loci. To facilitate visual depiction of the different scaling trends for each sample the LOESS regression is also shown along with slopes describing the major trends.

value for any given row and column combination represents the relative proportion of physical contacts made by the two corresponding genomic loci. A graphical representation of the data can be seen in Figure 1B and C. All of the features noted below were evident in a biological replicate of this experiment performed with lower sequence coverage.

The yeast genome undergoes large scale reorganization in quiescence

The basic higher-order chromatin organization in growing and quiescent cells can be seen in Figure 1B with the chromatin from both quiescent (orange) and exponentially growing (blue) cells adopting similar overall conformations. In agreement with previous Hi-C experiments performed on yeast and other organisms, cis (intra-chromosomal) interactions are much more frequent than trans (inter-chromosomal) interactions, suggesting compartmentalization of individual chromosomes within the nucleus (36–38). Moreover, cis interactions fall off exponentially with increasing distance between loci (Figure 2 and Supplementary Figure S1). The average levels of trans contacts for all chromosomes follow the previously reported trend (12) that chromosome size correlates inversely with trans interaction frequency on the whole (Supplementary Figure S2A), and contacts between smaller chromosome arms tend to be about twice as frequent as contacts between longer arms (Supplementary Figure S2B). These features are seen in both exponential growth and quiescence.

In terms of nuclear organization of the genome, the budding yeast chromosomes adopt a Rabl-like conformation where the centromeres are held securely near the nuclear periphery close to the spindle pole body by kinetochore microtubule attachments, with chromosome arms splayed backward away from the centromeres and into the nuclear space (5–7,39). This organization is immediately apparent in our data as seen by strong interactions between all centromeric regions (defined as about 40 kb on either side of the centromere) but very few interactions between centromeric regions and chromosome arms. In fact, the interactions of centromeric regions with chromosome arms are the least frequent class of interactions in the data set suggesting a strongly maintained spatial compartmentalization of the two classes of genomic elements. Furthermore, this phenomenon appears to be maintained from exponential growth to quiescence suggesting that it is a fundamental aspect of nuclear organization in budding yeast (Figure 1B).

Figure 1C provides a differential view of the chromatin organization between quiescent cells and exponentially growing cells. Three striking features are apparent from this graph. The first feature is the dramatic increase in long range cis interactions at the expense of short range interactions in quiescent cells. Excluding peri-centromeric and subtelomeric regions, loci that are closer than 40 kb interact much more frequently in exponentially growing cells than in quiescent cells. In contrast, loci spaced further apart than 40 kb are much more likely to interact during quiescence than during exponential growth. Figure 2 and Supplementary Figure S1 provide summaries of how the chromosome polymers' self-interactions scale with distance for both states and document that this shift in short range to long range interactions in quiescence occurs over all chromosomes. This occurrence of a higher proportion of long-range cis contacts during quiescence is consistent with the hypothesis that the chromatin of quiescent cells is more compact than that of exponentially growing cells.

The second feature that is apparent from Figure 1C is the drastic decrease in interaction frequency among centromeric regions during quiescence. A condensed interaction matrix of centromeric regions can be seen in Figure 3A. Nearly all centromeric regions have moderate decreases in trans interaction frequency, and the changes are even more pronounced when considering only the genomic bins containing the centromeres. This is consistent with data described previously for cells transitioning from exponential growth to stationary phase (26). Even though the inter-centromeric interactions decline in quiescence, the cis interaction frequency between the two pericentric regions on either side of the centromere on each chromosome is maintained, highlighting the maintenance of the Rabl conformation of chromosomes from exponential growth to quiescence (Figure 1B). However, coincident with the decrease in trans interactions of the centromeres, the intra-chromosomal interactions between pericentric regions and the corresponding chromosome arms increase during quiescence (Supplementary Figure S3), likely reflecting a substantial disaggregation of the centromeric compartment of the nucleus resulting in increased opportunity for intrachromosomal interactions.

The third prominent feature of the comparative Hi-C data is the change in interaction frequency of the subtelomeric regions (defined as about 30 kb from the chromosome ends). Figures 1C and 3B show that, in contrast to the centromeric trend, most subtelomeric regions interact with

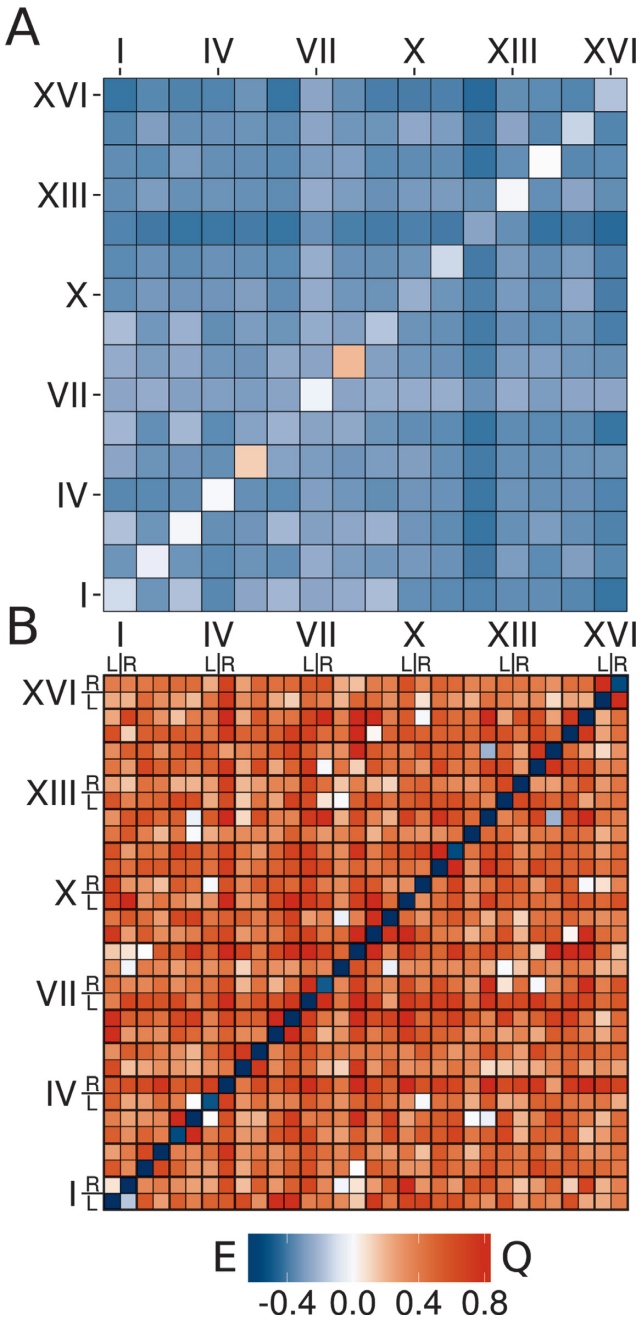

Figure 3. (**A**) Centromeric regions interact less frequently with each other during quiescence. Data values are taken from Figure 1C and condensed into individual bins representing the average interaction frequency for the centromeric regions, defined as a range spanning about 40 kb pairs on either side of the centromeres. Chromosomes are labeled periodically along the axes. (**B**) Subtelomeric regions interact more frequently with each other during quiescence. Data values are taken from Figure 1C and condensed into individual bins representing the average interaction frequency for the subtelomeric regions, defined as a range spanning about 30 kb pairs from the end of the chromosome. Chromosomes are labeled periodically along the axes with 'L' and 'R' representing the left and right subtelomeric regions for the corresponding chromosome, respectively.

each other much more frequently during quiescence both intra- and inter-chromosomally. In both exponential and quiescent cells, telomeres on arms of equal length interact more frequently than those of unequal length (Supplementary Figure S4). Telomeres form 4–8 foci within the nucleus during exponential growth (7–8,40). Thus, hypotheses consistent with our data are that these telomere clusters are consolidated into fewer foci during quiescence or that the foci persist for a longer duration. To test these hypotheses, we measured the number of telomeric foci in exponential versus quiescent cells by fluorescence microscopy of a prototrophic strain expressing Rap1-GFP. As noted in Supplementary Figure S5A,D, the number of telomeric foci actually increases in quiescence in cells starved for either glucose or nitrogen. However, the intensity of Rap1 staining at the foci increased in quiescent cells, suggesting that a larger amount of Rap1 was incorporated into telomeric domains upon entry into quiescence (Supplementary Figure S5C,D), perhaps as a consequence of being liberated from ribosomal protein and ribosomal biogenesis gene promoters. These observations are consistent with more sites of telomere interaction but more robust interaction at those sites.

Organization of several functional genomic elements remains essentially unchanged in quiescence

rDNA and the nucleolus. In both exponentially growing and quiescent cells, the rDNA locus constitutes a profound barrier dividing chromosome XII into two distinct domains that exhibit almost no interactions between sites on the two separate domains (Figures 1C and 4). Thus, even though rDNA expression is substantially decreased in quiescent cells (41–44), the nuclear organization of chromosome XII retains its distinct topological domains, indicating that the nucleolus remains essentially intact. This is consistent with previous cytological observations that the rDNA undergoes increased compaction dependent on condensin upon nutrient starvation (45). We note that the longer range intrachromosomal interactions in quiescent cells increase among sites within each domain of chromosome XII, to a greater distance and a greater frequency than those on other chromosome arms. Thus, the reduced nucleolar volume in quiescent cells may allow greater flexibility of the DNA attached to the organelle.

Origins of replication. A number of observations suggest that origins of replication, essentially equivalent to autonomously replicating sequences (ARSs), associate during exponential growth (46). Current data suggest that a limited number of 'replication factories' exist within the cell and that DNA strands are pulled through those factories during replication. The most compelling evidence for such factories is derived from observations from Tanaka's group, who showed that sites equidistant on either side of an ARS converge during replication and then disperse after replication (16). Since quiescent cells no longer undergo replication and thus replication factories would not be expected to be active, we were interested in addressing whether ARS elements exhibited reduced 3D associations in quiescence. Accordingly, we examined specifically the change in interactions of ARSs under this transition. As seen in Figure 5,

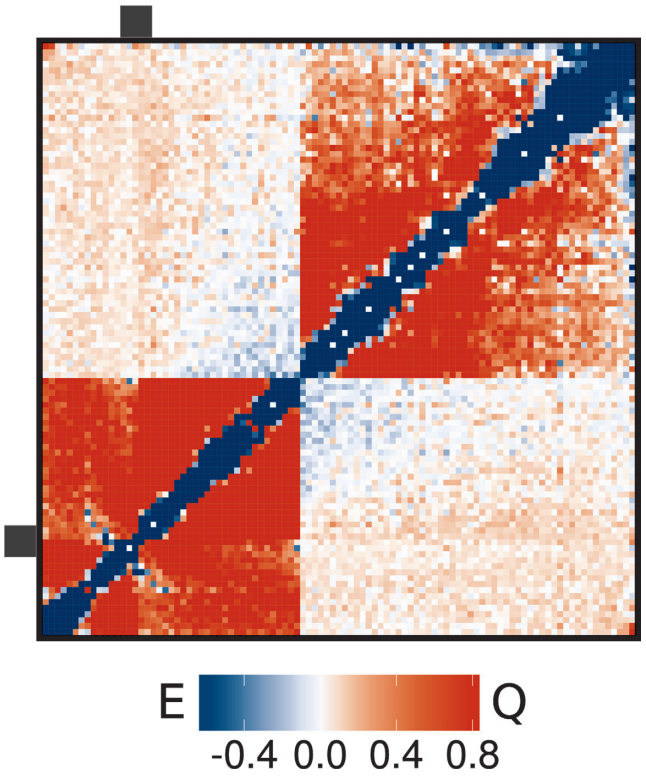

Figure 4. The rDNA spatially segregates the right arm of chromosome XII. Chromosome XII highlighted from Figure 1C. Relative to the rDNA located near the middle of chromosome XII, the centromere-proximal side of the chromosome shows very few interactions with the centromere-distal side. Furthermore, in both growth states each side of the chromosome shows a higher self-interaction frequency than do most other chromosome arms with an even greater increase during quiescence.

some ARS domains show a decrease in association in quiescent relative to growing cells while others show an increase in interaction. Interestingly, when replication origins are queried by their firing time during S phase (47) a subset of the earliest firing origins shows a large decrease in trans interaction frequency during quiescence (Figure 5). This is likely due to their close proximity to centromeres, which are known to be near some of the earliest firing origins apparently as a means of efficiently achieving biorientation of sister chromatids during S phase (48). Consistent with the overall changes in topological organization, the ARS domains showing a decrease in association are those located in peri-centric regions, whose trans interactions, as noted above, are dispersed during quiescence. Thus, the reorganization of ARSs during quiescence appears primarily to be a consequence of the dispersion of peri-centromeric regions rather than dissociation of specific replication factories.

tRNA genes. Thompson et al. (13) showed by fluorescence *in situ* hybridization that several groups of tRNA family genes were clustered near the periphery of the nucleolus. Moreover, Duan et al. suggested from earlier Hi-C studies that most tRNA genes participate in one of two interaction groups during exponential growth, one of which appeared to be associated with the rDNA locus (12). Our results at higher resolution with exponentially growing cells confirm

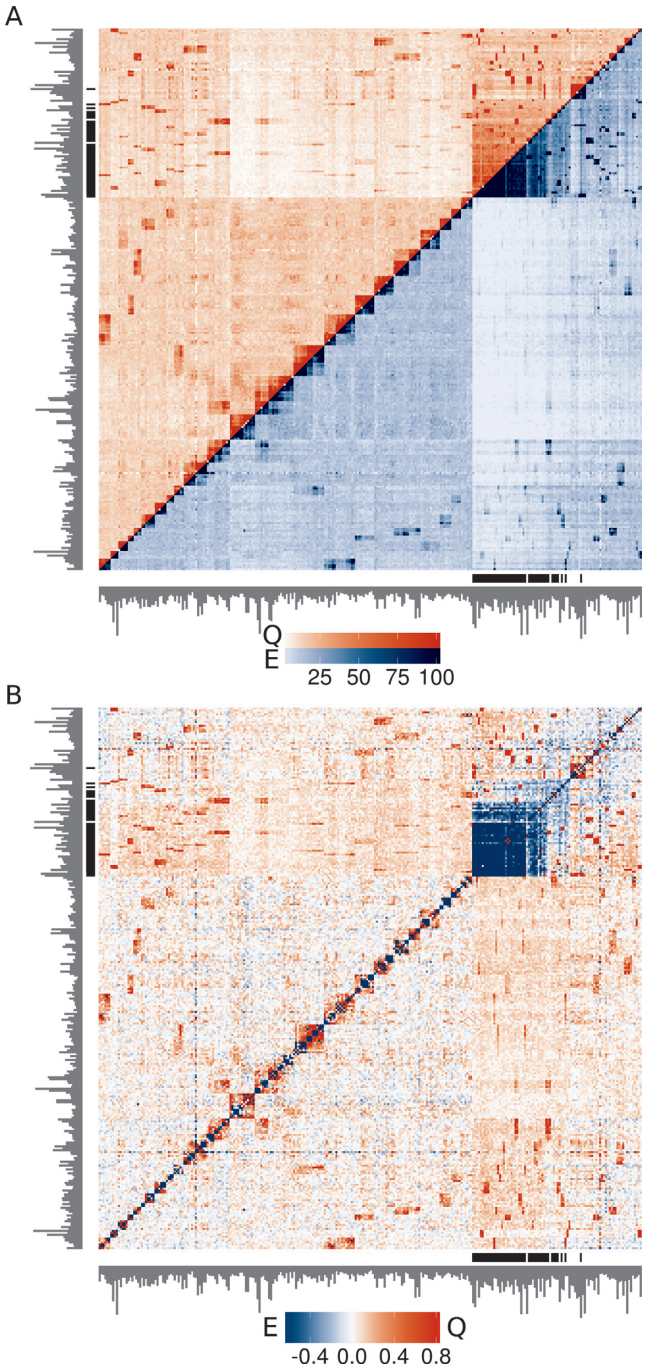

Figure 5. Autonomous Replication Sequences cluster into distinct functional groups. Data for those bins containing ARS elements were organized by unsupervised hierarchical clustering of the exponential growth data and shown in (**A**) for quiescent (top left, orange) and exponentially growing (bottom right, blue) cells and in (**B**) for the difference between the two data sets. Pericentric ARSs are marked by black dashes along the axes, and the replication timing of each ARS is given by the gray bars along the axes (bar length represents the percent of cells that have replicated the ARS 10 min after the start of S phase). Pericentric ARSs and early-firing origins tend to cluster together in the upper-right cluster with pericentric ARSs showing greatly decreased interaction frequency during quiescence. Trans interactions between clusters generally increase during quiescence while cis interactions other than those involving the pericentric ARSs show little change on average. Smaller clusters form from ARSs along the same chromosome.

the pattern reported in that earlier study but point to a different mechanistic basis for that clustering (Figure 6A). In particular, we note strong association among a core of approximately 64 tRNA genes comprising an aggregate of local clusters of tRNA genes near the centromeres of all the chromosomes. The genes defined by Thompson et al. as residing near the nucleolus are equally distributed among this core cluster and regions not in the core. Moreover, the tRNA gene 12tQ(UUG)L, located less than 3 kb from the rDNA cluster, does not show any notable trans association with any other tRNA genes. On a larger scale, all tRNA genes fall into one of two groups of approximately equal numbers, one of which comprises genes that show little interaction with the pericentric core tRNA genes (Figure 6A, lower left quadrant) and one comprising genes that interact more extensively with that core group (upper right quadrant). Finally, tRNA genes exhibit enhanced intrachromosomal interactions over all the chromosome arms, but with all the tRNAs on chromosome X showing quite high interaction across the entire chromosome. We conclude that the major organizing principle of tRNA genes during exponential growth is the overall chromosomal structure imposed by centromere clustering and the persistent Rabl configuration, with any potential higher order organization masked by this predominant signal.

This overall pattern of tRNA organization remains unchanged in quiescent cells, although the intensities of the interactions do change (Figure 6A and B). In particular, the pericentric tRNA genes in the core cluster interact less frequently in quiescence than in exponential growth. On the other hand, more distant tRNA genes on the same chromosome interact more frequently in quiescent cells than in growing cells, often at the expense of shorter distance interactions. Thus, the basic principles distinguishing the change in the overall organization of the genome in quiescence drive the observed changes in the organization of tRNA genes.

Confirmation of Hi-C results by interrogation of individual loci

Our Hi-C results spark several predictions regarding the relative intracellular arrangements of specific regions of the genome. In order to test those predictions, we used fluorescence microscopy as an orthogonal approach to measure spatial distances between loci (49,50). Our assumption is that an increased frequency of interaction reflects a decreased average distance between the interacting loci. In order to measure the distance between two loci, we inserted a large array of Lac operator repeats and a large array of Tet operator repeats into two different loci in strains expressing GFP-tagged Lac repressor and mCherry-tagged Tet repressor. The binding of the fluorescent repressors to their respective operators produced two distinct colored spots in the microscope, from which by analyzing deconvolved z-stacks we could calculate a 3D separation distance in a large number of individual cells.

One conclusion from the Hi-C results is that many telomeres spend more time in close association in quiescence than during active growth. Accordingly, we measured the distribution of distances in individual exponentially growing cells

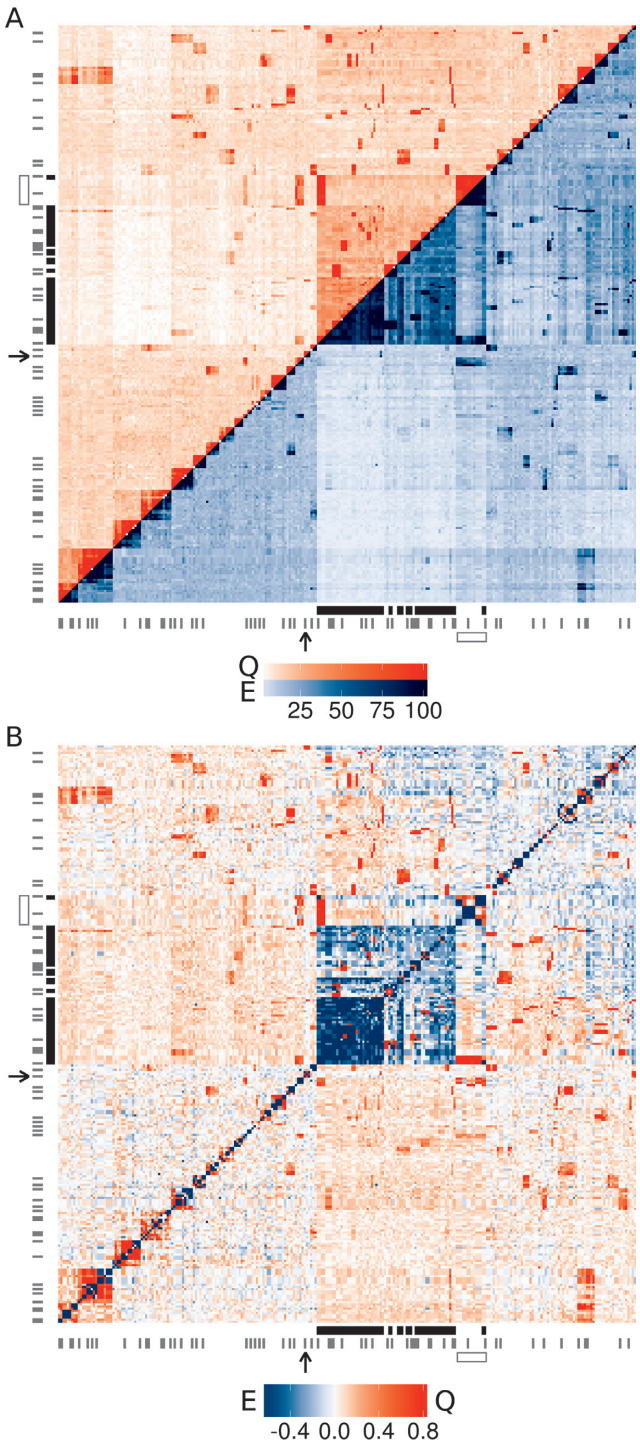

Figure 6. tRNAs partition into two large groups. Unsupervised hierarchical clustering of the exponential growth data was applied to the tRNA data shown for (**A**) quiescent (top left, orange) and exponentially growing (bottom right, blue) cells and (**B**) the differential data set. Pericentric tRNAs are marked by black dashes along the axes, and tRNAs previously identified to be localized near the nucleolus are marked with gray dashes along the axes. Pericentric tRNAs cluster together in the upper-right cluster and show large decreases in interaction frequency during quiescence, while nucleolar tRNAs are spread throughout both large clusters. Trans interactions between clusters generally increase during quiescence while cis interactions other than those involving the pericentric tRNAs show little change on average. Smaller clusters form from tRNAs along the same chromosome.

compared to those in quiescent cells for three sets of loci: TEL09R versus TEL03L, TEL09R versus TEL03R and TEL09R versus TEL09L. Our Hi-C data indicated an increased interaction for all three of these pairs in quiescence. Consistent with this observation, our microscopy analysis returned a mean distance between loci in quiescent cells of 6.1%, 7.3% and 5.8% shorter in quiescent than in exponentially growing cells, respectively, a modest but statistically relevant difference (Figure 7). Thus, the increased frequency of interaction correlates with a decreased average inter-loci distance. As noted above, this reduced distance does not derive from fewer telomeric foci in quiescent cells. Rather, more telomeric foci are present in quiescent cells than in growing cells, albeit with an apparent increase in Rap1 abundance at those foci, suggesting a possible increase in the avidity of the interactions.

A second observation from our Hi-C results is an increase in long range intrachromosomal interactions in quiescent cells relative to that in growing cells. To confirm this, we inserted the *Tet*O array upstream of *HOP1* and the *Lac*O array upstream of *TAO3*, thereby positioning them 119 kb apart on the same arm of chromosome IX. Figure 8A presents representative images of cells imaged for these arrays. Figure 8B reports the cumulative distances between the two spots in a wild type background grown at 23°C exponentially or starved for glucose or nitrogen. For the exponential growth and glucose-starved conditions the cultures were split once reaching the appropriate cell density, with one subset staying at 23°C and the other shifted to 37°C for 3 h. Three biological replicates were examined for each condition and more than 500 cells imaged and analyzed for each replicate. As evident, the distance between the loci in exponentially growing cells was on average significantly longer than that in the quiescent cells obtained at either temperature or by starvation for either glucose or nitrogen ($P < 0.05$ in all cases). In a separate experiment with cells grown or starved at 30°C, the distance between the loci was also significantly shorter in quiescent cells ($P = 2\times10^{-8}$, data not shown). These results are consistent with the hypothesis that quiescent cells exhibit a higher average degree of chromosome condensation than do growing cells, which would account for the increased long range interactions observed by Hi-C and the shorter intrachromosomal distance detected by microscopic observation.

As an initial step in addressing the molecular basis for the increased chromatin compaction during quiescence, we first asked whether the nuclear volume was reduced in cells in quiescence relative to that in exponential growth. We observed no difference in the volume of quiescent cells obtained by glucose starvation although quiescent cells obtained by nitrogen starvation did have smaller nuclei (Supplementary Figure S5B). Accordingly, while the reduced nuclear volume of the nitrogen starved cells might contribute to the observed chromosome compaction, it does not account for compaction in glucose starved cells. We next examined the effect on compaction of inactivating either the cohesin or the condensin complex. To do so, we grew at 23°C a prototrophic wild type strain carrying arrays at *HOP1* and *TAO3* as described above as well as identical strains carrying a temperature sensitive allele in the gene encoding one subunit of the cohesin complex, *smc1–2*, or in the gene encoding one of the subunits of the condensin complex, *smc2–8*, and then induced cells into quiescence by glucose starvation for one day. We split the cultures and incubated one half at 23°C and the other half at 37°C for 3 h, at which point we harvested cells and measured the distances between the two chromosome markers in more than 1000 cells for each culture under each condition. In addition, we measured the inter-marker distance in the three strains in exponential growth both at 23°C and 3 h after incubation at 37°C. As shown in Figure 8C, inactivation of *SMC1* in cells in exponential phase or quiescence did not comparatively affect the distance between the two loci in a manner that would indicate involvement of cohesin in the differences in condensation between the two growth states. In contrast, inactivation of *SMC2* resulted in a small but statistically significant increase in the distance between the loci in exponentially growing cells—median distance of 0.62 μm versus 0.55 μm. More noteworthy, inactivation of *SMC2* in quiescent cells substantially expanded the distance between the two loci in approximately 30% of cells (Figure 8D). These results suggest that complete compaction of chromosomes in quiescence depends on the condensin but not the cohesin complex.

DISCUSSION

We have examined the changes in 3D organization of the genome that yeast cells undergo in the transition from exponential growth to quiescence. We observe three major differences in the organization of the quiescent cell genome relative to that in growing cells that are illustrated in Figure 9. First, we find an increased frequency of intrachromosomal associations at longer distances in quiescence than in growing cells. Second, we observe a decrease in inter-centromeric interactions. Third, we find an increase in inter-telomeric interactions. These changes point to pronounced remodeling of the genomic topology that occurs on entry into quiescence.

Our Hi-C results demonstrate a universal increase in the frequency of more distant intrachromosomal interactions, roughly greater than 40 kb, relative to that of shorter range interactions. Moreover, direct measurement of distance between distant loci on the same chromosome indicates a highly significant decrease in quiescent cells, regardless of the means by which they were induced into quiescence, consistent with an increase in the frequency of interaction of distant loci. Our current understanding of chromatin organization postulates several levels of DNA compaction, with the first level consisting of DNA wound around nucleosomes to yield 'beads on a string.' The second level, which observational and computation data support, results from compaction of nucleosomes into a quasi-random zigzag pattern to yield 30 nm fibers (51). The next level, for which limited experimental data exist, has been hypothesized to consist of loops arising as though the 30 nm fibers were reeled in hand-over-hand, yielding an inner attachment core fiber where the hands grip the DNA with the loops emanating outward to form 'topologically associated domains' (52). One possible explanation of our data in this study could be that the length of these loops are longer in quiescent cells; that is, that the distance between the attach-

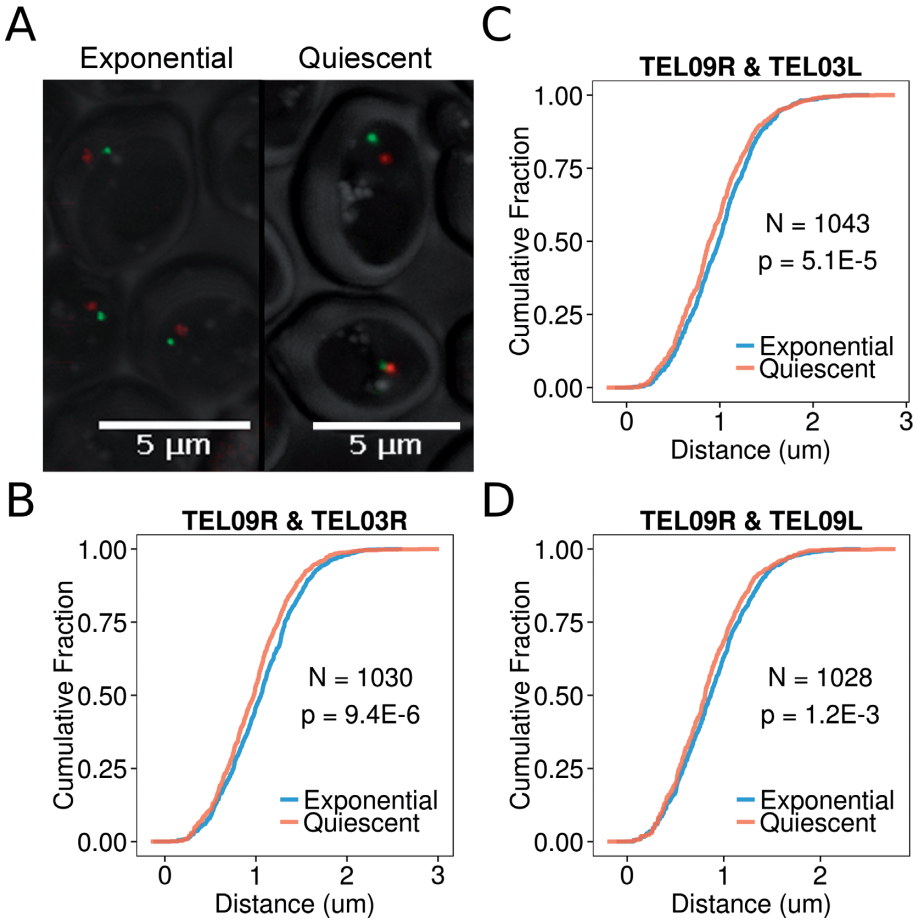

Figure 7. Subtelomeric regions have shorter 3D separation distances in quiescent cells. (**A**) An example of microscopic measurement of separation distance between two subtelomeric loci in quiescent and exponentially growing cells. Green and red spots represent LacI-GFP and TetR-mCherry subtelomeric foci, respectively, while diffuse fluorescence around the foci outlines the nuclear volume (not depicted here so as to best visualize the foci). (**B**–**D**) Empirical cumulative distribution functions for the 3D distances between TEL09R and TEL03L (B), TEL09R and TEL03R (C) and TEL09R and TEL09L (D) in both growth states. At any given distance along the horizontal axis the fraction of cells with subtelomeric loci separated by a distance shorter than the given distance is given along the vertical axis. The Mann–Whitney *U*-test *P*-values are given for the null hypothesis that the two distributions are equal and the alternative hypothesis that the distribution for the exponentially growing cells is shifted to the right relative to that of the quiescent cells.

ment sites in the inner core are spaced more widely along the chromosome. A second explanation could be that the chromosomes are simply more 'scrunched up' due to the reduced distance they span between the centromeres located on the microtubule array and the nuclear envelope. Both models would concurrently yield an increase in distant interactions and a reduction in intrachromosomal distances, consistent with our observations. These results suggest several follow up experiments, including mapping genome-wide attachment sites in quiescent cells of condensin and related molecules responsible for this higher order organization of chromatin, particularly since we observe that condensin is required for chromosome compaction in quiescent cells.

The second major reorganization of the topology of the genome in quiescent cells is a dispersion of centromeres. This observation can be explained in the light of recent observations by Laporte, et al. (26) who showed that the yeast spindle undergoes a major reorganization in stationary phase. In particular, the cytoplasmic microtubules disappear and a long stable monopolar array of nuclear microtubules assembles from the single spindle pole body and spans the nucleus. While the kinetochores remain attached to the nuclear microtubules, they no longer sequester at the spindle pole body but distribute along the monopolar microtubule array. This would explain the reduction in interchromosomal interaction of centromeric regions, although the limited interaction of the centromeric region with arms of the same or other chromosomes remains low, suggesting a persistence of the Rabl configuration in quiescence.

The third major reorganization of the topology of the genome in quiescent cells is an increase in the interaction among telomeres. This is true for almost all pairwise telomere interactions, both inter- and intrachromosomal, and was confirmed by fluorescence microscopy for three separate pairs. During exponential growth, telomeres reside at the nuclear periphery in 4-8 foci with telomeres on the arms of chromosomes of roughly equal length exhibiting higher interaction (7–8,10–11,40). Our results are not the consequence of formation of fewer telomeric foci in the nucleus, since we in fact observe an increase in the number of foci in quiescent cells relative to growing cells. However, we note that the intensity of Rap1 binding at the foci is substantially

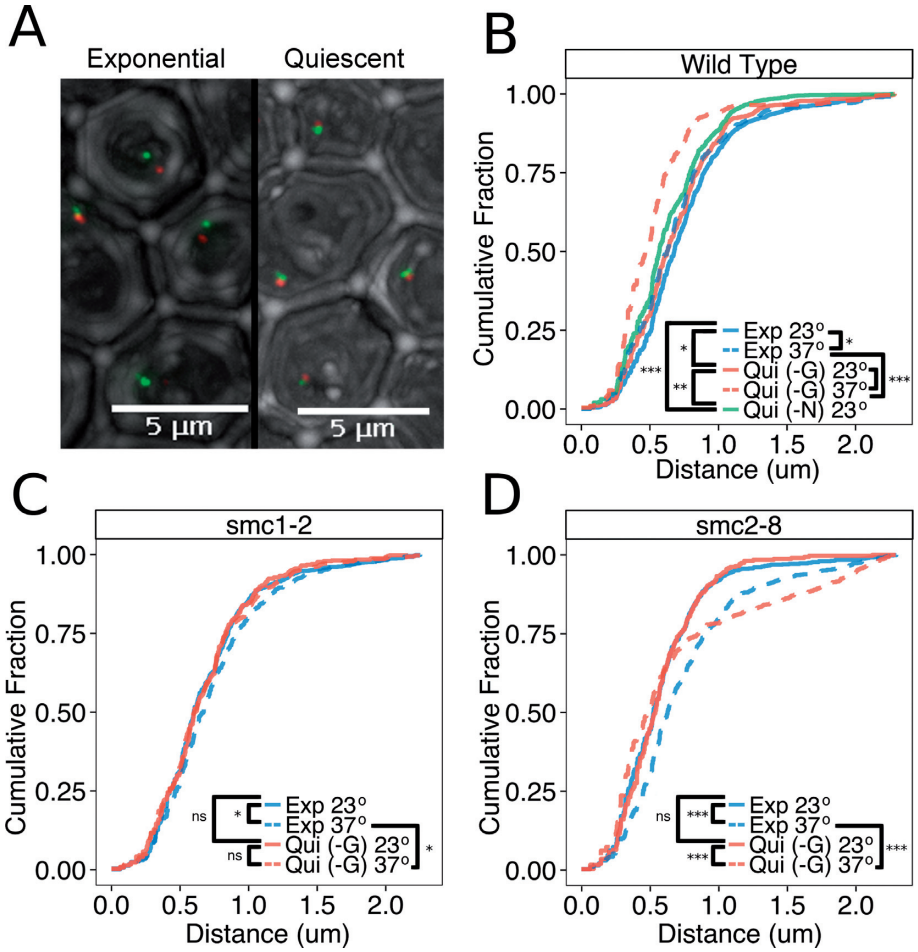

Figure 8. Two loci bounding a 119 kb region along chromosome IX have a shorter 3D separation distance in quiescent cells. (**A**) An example of microscopic measurement of separation distance between two loci that bound a 119 kb region along chromosome IX. Green and red spots represent *Lac*I-GFP and *Tet*R-mCherry foci, respectively, while diffuse fluorescence around the foci outlines the nuclear volume (not depicted here so as to best visualize the foci). (**B**) Empirical cumulative distribution function for the 3D distances between the loci in exponential growth ('Exp') at 23°C or following a 3 h shift to 37°C, 1-day glucose-starved quiescence ('Qui (-G)') at 23°C or starved at 23°C and then shifted to 37°C for 3 h, and 1-day nitrogen-starved quiescence at 23°C ('Qui (-N)'). Cells containing more than one red and one green spot were eliminated from consideration, as were cells with mitotic nuclei or with distances between spots greater than 2.3 µm. Three independent biological replicates gave essentially identical results and the data for all three experiments were pooled for the figure. The Kolmogorov–Smirnov test was performed under the null hypothesis that the two distributions are equivalent. *, $P < 0.05$; **, $P < 0.003$; ***, $P < 0.0001$. (**C**, **D**) Empirical cumulative distribution function for the 3D distances between the loci in strains carrying either temperature sensitive allele *smc1–2* (C) or *smc2–8* (D) in exponential growth ('Exp') at 23°C or following a 3 h shift to 37°C or 1-day glucose-starved quiescence ('Qui (-G)') at 23°C or starved at 23°C and then shifted to 37°C for 3 h. *P*-values were determined using the Kolmogorov–Smirnov test as above.

greater in quiescent cells than in growing cells. This could result from the liberation of Rap1 from the several hundred ribosomal biogenesis and ribosomal protein genes, whose expression declines significantly in the non-growing quiescent cells. Such an increase in binding could perhaps increase the strength, and thus the duration, of the intertelomeric interactions within the foci.

We note that a variety of functionally related genomic features, including tRNA genes, origins of replication and Ty elements (Supplementary Figure S6), show no specific interactions either during exponential growth or during quiescence or change their interactions on the transition from one state to the other. While we do detect variation in the aggregation of subsets of each group of elements during exponential growth, this aggregation can be accounted for solely on the basis of the close association of pericentric regions of all chromosomes during exponential growth and the reduction of that association during quiescence. This is somewhat surprising for tRNA genes in light of previous results from fluorescence *in situ* hybridization that at least a subset of tRNA genes associate with the periphery of the nucleolus (13). A previous Hi-C experiment seemed to confirm that association (12). However, our results obtained at a significantly higher resolution fail to confirm those earlier studies and suggest that these earlier results may have mistaken the pericentric association for functional organization.

One rationale for examining the higher order organization of chromatin in quiescent yeast cells was the prior observation by Piñon of a distinct chromatin body in quiescent versus exponentially growing cells. This G0 genome sedimented at a slower rate in sucrose gradients than genomes from either G1 or G2 cells. This would suggest that the G0 chromatin body contained either less mass than that from G1or G2 cells or that it occupied more volume. Our re-

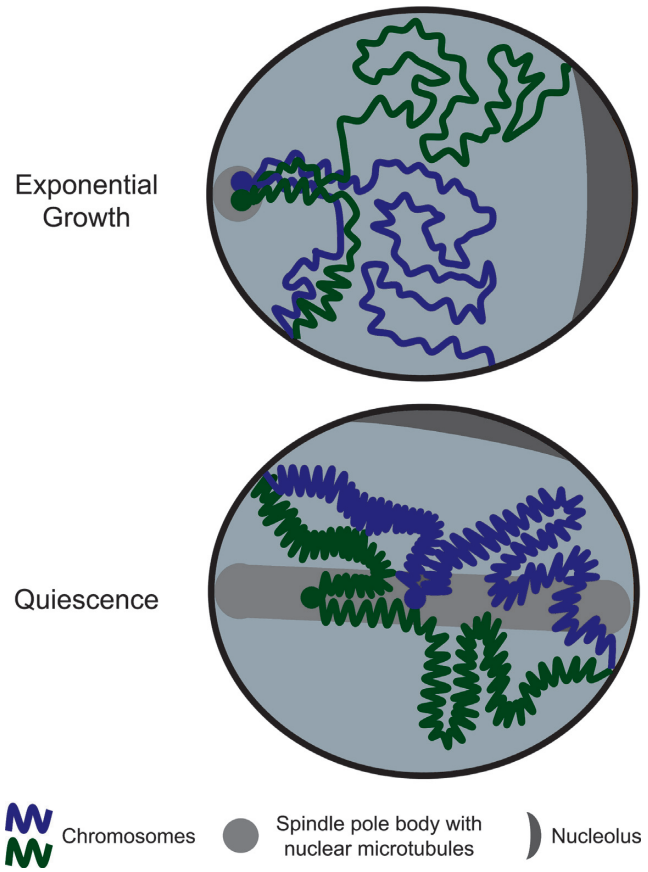

Figure 9. Model of genome topology in growing and quiescent yeast cells. During exponential growth centromeres aggregate at the spindle pole body on one side of the nucleus with the nucleolus on the opposite side. The arms of each chromosome associate in the pericentric region but then splay outward into the nuclear space with the ends of the chromosomes forming 4–8 foci at the nuclear periphery. Each chromosome interacts on average with itself more often than it does with other chromosomes. The smaller chromosome arms interact with each other more than they do with the larger chromosome arms. During quiescence, centromeres distribute along an array of nuclear microtubules that spans the nucleus and thus interact much less frequently with each other but remain functionally compartmentalized away from other regions of the genome. Conversely, telomeres interact with each other more frequently, possibly due to an increased propensity for telomeres to participate in foci or an increased duration of association in foci. Moreover, longer range intra-chromosomal interactions increase at the expense of those at shorter range likely as a consequence of increased compaction of the chromosomes.

sults suggesting that the chromatin in quiescent cells is more compacted than that of exponentially growing cells does not account for Piñon's observation. Rather, the dispersion of chromosomes along the novel quiescent microtubule bundle might be responsible for the increased volume of the chromatin body and the resulting reduced sedimentation rate. Our results demonstrating a reduced interchromosomal interaction of centromeres adds weight to the hypothesis.

The observations from this study raise two interrelated questions: what is responsible for the reorganization of the yeast genome in quiescent cells and are those changes necessary for the survival of cells during quiescence? One way to address both questions is to determine what genes are required for the reorganization and do mutations in those genes reduce the survival of quiescent cells. We have shown that condensin is required for maintenance of chromatin compaction in quiescence, although we don't yet know whether this loss of compaction results in decreased viability in quiescence. The previous study by Laporte et al. examined the role of several microtubule associated proteins in formation of nuclear microtubule arrays in quiescence and the effect of mutations of genes encoding these proteins on survival in stationary phase. They found that the kinesin Kip3 and subunits of the dynactin complex were required for both nuclear microtubule formation and survival in quiescence. We would anticipate that these mutants would also be defective in at least a portion of the topological changes in quiescence we observe. We note that a number of genes involved in chromatin structure, including histone modifying enzymes *HAT1* and *RTT109*, exhibit reduced expression in quiescence. In addition, our prior studies identified a number of genes required for survival during long term starvation for glucose. These included a number of genes involved in chromatin structure such as *SPT4, IES2* and *ASF1,* the latter of which is required for long range interactions of sites on chromosome III (53). Accordingly, testing the effect of mutations in these genes on chromatin structure in quiescence would be informative.

The results presented here provide a possible common feature of quiescent cells that is assumed regardless of the means of entry into quiescence. We have found this feature is common to cells induced into quiescence by two different starvation regimens. Moreover, the extent to which some or all of these changes reflect essential components of quiescence in mammalian cells, such as memory B and resting T cells or certain stem cell populations, could prove productive lines of investigation.

ACCESSION NUMBERS

The Sequence Read Archive (SRA) accession number for the Hi-C data reported in this paper is SRP053245.

SUPPLEMENTARY DATA

Supplementary Data are available at NAR Online.

FUNDING

National Institutes of Health [GM076562 to J.R.B., HG003143 to J.D.]. Funding for open access charge: NIH [GM076562 to J.R.B.].
Conflict of interest statement. None declared.

REFERENCES

1. Cremer,T. and Cremer,C. (2001) Chromosome territories, nuclear architecture and gene regulation in mammalian cells. *Nat. Rev. Genet.*, **2**, 292–301.
2. Rouquette,J., Cremer,C., Cremer,T. and Fakan,S. (2010) Functional nuclear architecture studied by microscopy: present and future. *Int. Rev. Cell Mol. Biol.*, **282**, 1–90.
3. Chandra,T., Ewels,P.A., Schoenfelder,S., Furlan-Magaril,M., Wingett,S.W., Kirschner,K., Thuret,J.Y., Andrews,S., Fraser,P. and Reik,W. (2015) Global reorganization of the nuclear landscape in senescent cells. *Cell Rep.*, **10**, 471–483.

4. Taddei,A. and Gasser,S.M. (2012) Structure and function in the budding yeast nucleus. *Genetics*, **192**, 107–129.
5. Guacci,V., Hogan,E. and Koshland,D. (1997) Centromere position in budding yeast: evidence for anaphase A. *Mol. Biol. Cell*, **8**, 957–972.
6. Heun,P., Laroche,T., Shimada,K., Furrer,P. and Gasser,S.M. (2001) Chromosome dynamics in the yeast interphase nucleus. *Science*, **294**, 2181–2186.
7. Jin,Q., Trelles-Sticken,E., Scherthan,H. and Loidl,J. (1998) Yeast nuclei display prominent centromere clustering that is reduced in nondividing cells and in meiotic prophase. *J. Cell Biol.*, **141**, 21–29.
8. Palladino,F., Laroche,T., Gilson,E., Axelrod,A., Pillus,L. and Gasser,S.M. (1993) SIR3 and SIR4 proteins are required for the positioning and integrity of yeast telomeres. *Cell*, **75**, 543–555.
9. Bystricky,K., Laroche,T., van Houwe,G., Blaszczyk,M. and Gasser,S.M. (2005) Chromosome looping in yeast: telomere pairing and coordinated movement reflect anchoring efficiency and territorial organization. *J. Cell Biol.*, **168**, 375–387.
10. Schober,H., Kalck,V., Vega-Palas,M.A., Van Houwe,G., Sage,D., Unser,M., Gartenberg,M.R. and Gasser,S.M. (2008) Controlled exchange of chromosomal arms reveals principles driving telomere interactions in yeast. *Genome Res.*, **18**, 261–271.
11. Therizols,P., Duong,T., Dujon,B., Zimmer,C. and Fabre,E. (2010) Chromosome arm length and nuclear constraints determine the dynamic relationship of yeast subtelomeres. *Proc. Natl. Acad. Sci. U.S.A.*, **107**, 2025–2030.
12. Duan,Z., Andronescu,M., Schutz,K., McIlwain,S., Kim,Y.J., Lee,C., Shendure,J., Fields,S., Blau,C.A. and Noble,W.S. (2010) A three-dimensional model of the yeast genome. *Nature*, **465**, 363–367.
13. Thompson,M., Haeusler,R.A., Good,P.D. and Engelke,D.R. (2003) Nucleolar clustering of dispersed tRNA genes. *Science*, **302**, 1399–1401.
14. Wang,L., Haeusler,R.A., Good,P.D., Thompson,M., Nagar,S. and Engelke,D.R. (2005) Silencing near tRNA genes requires nucleolar localization. *J. Biol. Chem.*, **280**, 8637–8639.
15. Hiraga,S., Hagihara-Hayashi,A., Ohya,T. and Sugino,A. (2005) DNA polymerases alpha, delta, and epsilon localize and function together at replication forks in Saccharomyces cerevisiae. *Genes Cells*, **10**, 297–309.
16. Kitamura,E., Blow,J.J. and Tanaka,T.U. (2006) Live-cell imaging reveals replication of individual replicons in eukaryotic replication factories. *Cell*, **125**, 1297–1308.
17. Ohya,T., Kawasaki,Y., Hiraga,S., Kanbara,S., Nakajo,K., Nakashima,N., Suzuki,A. and Sugino,A. (2002) The DNA polymerase domain of pol(epsilon) is required for rapid, efficient, and highly accurate chromosomal DNA replication, telomere length maintenance, and normal cell senescence in Saccharomyces cerevisiae. *J. Biol. Chem.*, **277**, 28099–28108.
18. Pasero,P., Braguglia,D. and Gasser,S.M. (1997) ORC-dependent and origin-specific initiation of DNA replication at defined foci in isolated yeast nuclei. *Genes Dev.*, **11**, 1504–1518.
19. Gray,J.V., Petsko,G.A., Johnston,G.C., Ringe,D., Singer,R.A. and Werner-Washburne,M. (2004) 'Sleeping beauty': quiescence in Saccharomyces cerevisiae. *Microbiol. Mol. Biol. Rev.*, **68**, 187–206.
20. Broach,J.R. (2012) Nutritional control of growth and development in yeast. *Genetics*, **192**, 73–105.
21. Klosinska,M.M., Crutchfield,C.A., Bradley,P.H., Rabinowitz,J.D. and Broach,J.R. (2011) Yeast cells can access distinct quiescent states. *Genes Dev.*, **25**, 336–349.
22. Lu,C., Brauer,M.J. and Botstein,D. (2009) Slow growth induces heat-shock resistance in normal and respiratory-deficient yeast. *Mol. Biol. Cell*, **20**, 891–903.
23. Allen,C., Buttner,S., Aragon,A.D., Thomas,J.A., Meirelles,O., Jaetao,J.E., Benn,D., Ruby,S.W., Veenhuis,M., Madeo,F. *et al.* (2006) Isolation of quiescent and nonquiescent cells from yeast stationary-phase cultures. *J. Cell Biol.*, **174**, 89–100.
24. Pinon,R. (1978) Folded chromosomes in non-cycling yeast cells: evidence for a characteristic g0 form. *Chromosoma*, **67**, 263–274.
25. Lohr,D. and Ide,G. (1979) Comparison on the structure and transcriptional capability of growing phase and stationary yeast chromatin: a model for reversible gene activation. *Nucleic Acids Res.*, **6**, 1909–1927.
26. Laporte,D., Courtout,F., Salin,B., Ceschin,J. and Sagot,I. (2013) An array of nuclear microtubules reorganizes the budding yeast nucleus during quiescence. *J. Cell Biol.*, **203**, 585–594.
27. Amberg,D.C., Burke,D.J. and Strathern,J.N. (2005) *Methods in Yeast Genetics: A Cold Spring Harbor Laboratory Course Manual, 2005 Edition*. Cold Spring Harbor Laboratory Press, Cold Spring Harbor, NY.
28. Simon,P., Houston,P. and Broach,J. (2002) Directional bias during mating type switching in Saccharomyces is independent of chromosomal architecture. *EMBO J.*, **21**, 2282–2291.
29. Gard,S., Light,W., Xiong,B., Bose,T., McNairn,A.J., Harris,B., Fleharty,B., Seidel,C., Brickner,J.H. and Gerton,J.L. (2009) Cohesinopathy mutations disrupt the subnuclear organization of chromatin. *J. Cell Biol.*, **187**, 455–462.
30. Schneider,C.A., Rasband,W.S. and Eliceiri,K.W. (2012) NIH Image to ImageJ: 25 years of image analysis. *Nat. Methods*, **9**, 671–675.
31. Linkert,M., Rueden,C.T., Allan,C., Burel,J.M., Moore,W., Patterson,A., Loranger,B., Moore,J., Neves,C., Macdonald,D. *et al.* (2010) Metadata matters: access to image data in the real world. *J. Cell Biol.*, **189**, 777–782.
32. Belton,J.M., McCord,R.P., Gibcus,J.H., Naumova,N., Zhan,Y. and Dekker,J. (2012) Hi-C: a comprehensive technique to capture the conformation of genomes. *Methods*, **58**, 268–276.
33. Lang,G.I., Parsons,L. and Gammie,A.E. (2013) Mutation rates, spectra, and genome-wide distribution of spontaneous mutations in mismatch repair deficient yeast. *G3 (Bethesda)*, **3**, 1453–1465.
34. Langmead,B. and Salzberg,S.L. (2012) Fast gapped-read alignment with Bowtie 2. *Nat. Methods*, **9**, 357–359.
35. Imakaev,M., Fudenberg,G., McCord,R.P., Naumova,N., Goloborodko,A., Lajoie,B.R., Dekker,J. and Mirny,L.A. (2012) Iterative correction of Hi-C data reveals hallmarks of chromosome organization. *Nat. Methods*, **9**, 999–1003.
36. Lieberman-Aiden,E., van Berkum,N.L., Williams,L., Imakaev,M., Ragoczy,T., Telling,A., Amit,I., Lajoie,B.R., Sabo,P.J., Dorschner,M.O. *et al.* (2009) Comprehensive mapping of long-range interactions reveals folding principles of the human genome. *Science*, **326**, 289–293.
37. Dixon,J.R., Selvaraj,S., Yue,F., Kim,A., Li,Y., Shen,Y., Hu,M., Liu,J.S. and Ren,B. (2012) Topological domains in mammalian genomes identified by analysis of chromatin interactions. *Nature*, **485**, 376–380.
38. Mizuguchi,T., Fudenberg,G., Mehta,S., Belton,J.M., Taneja,N., Folco,H.D., FitzGerald,P., Dekker,J., Mirny,L., Barrowman,J. *et al.* (2014) Cohesin-dependent globules and heterochromatin shape 3D genome architecture in S. pombe. *Nature*, **516**, 432–435.
39. Dekker,J., Rippe,K., Dekker,M. and Kleckner,N. (2002) Capturing chromosome conformation. *Science*, **295**, 1306–1311.
40. Gotta,M., Laroche,T., Formenton,A., Maillet,L., Scherthan,H. and Gasser,S.M. (1996) The clustering of telomeres and colocalization with Rap1, Sir3, and Sir4 proteins in wild-type Saccharomyces cerevisiae. *J. Cell Biol.*, **134**, 1349–1363.
41. Merz,K., Hondele,M., Goetze,H., Gmelch,K., Stoeckl,U. and Griesenbeck,J. (2008) Actively transcribed rRNA genes in S. cerevisiae are organized in a specialized chromatin associated with the high-mobility group protein Hmo1 and are largely devoid of histone molecules. *Genes Dev.*, **22**, 1190–1204.
42. Sandmeier,J.J., French,S., Osheim,Y., Cheung,W.L., Gallo,C.M., Beyer,A.L. and Smith,J.S. (2002) RPD3 is required for the inactivation of yeast ribosomal DNA genes in stationary phase. *EMBO J.*, **21**, 4959–4968.
43. Wittner,M., Hamperl,S., Stockl,U., Seufert,W., Tschochner,H., Milkereit,P. and Griesenbeck,J. (2011) Establishment and maintenance of alternative chromatin States at a multicopy gene locus. *Cell*, **145**, 543–554.
44. Philippi,A., Steinbauer,R., Reiter,A., Fath,S., Leger-Silvestre,I., Milkereit,P., Griesenbeck,J. and Tschochner,H. (2010) TOR-dependent reduction in the expression level of Rrn3p lowers the activity of the yeast RNA Pol I machinery, but does not account for the strong inhibition of rRNA production. *Nucleic Acids Res.*, **38**, 5315–5326.
45. Tsang,C.K., Li,H. and Zheng,X.S. (2007) Nutrient starvation promotes condensin loading to maintain rDNA stability. *EMBO J.*, **26**, 448–458.
46. Newport,J. and Yan,H. (1996) Organization of DNA into foci during replication. *Curr. Opin. Cell Biol.*, **8**, 365–368.

47. Alvino,G.M., Collingwood,D., Murphy,J.M., Delrow,J., Brewer,B.J. and Raghuraman,M.K. (2007) Replication in hydroxyurea: it's a matter of time. *Mol. Cell Biol.* **27**, 6396–6406.
48. Feng,W., Bachant,J., Collingwood,D., Raghuraman,M.K. and Brewer,B.J. (2009) Centromere replication timing determines different forms of genomic instability in Saccharomyces cerevisiae checkpoint mutants during replication stress. *Genetics*, **183**, 1249–1260.
49. Robinett,C.C., Straight,A., Li,G., Willhelm,C., Sudlow,G., Murray,A. and Belmont,A.S. (1996) In vivo localization of DNA sequences and visualization of large-scale chromatin organization using lac operator/repressor recognition. *J. Cell Biol.*, **135**, 1685–1700.
50. Straight,A.F., Belmont,A.S., Robinett,C.C. and Murray,A.W. (1996) GFP tagging of budding yeast chromosomes reveals that protein-protein interactions can mediate sister chromatid cohesion. *Curr. Biol.*, **6**, 1599–1608.
51. Grigoryev,S.A. and Woodcock,C.L. (2012) Chromatin organization - the 30 nm fiber. *Exp. Cell Res.*, **318**, 1448–1455.
52. Bickmore,W.A. and van Steensel,B. (2013) Genome architecture: domain organization of interphase chromosomes. *Cell*, **152**, 1270–1284.
53. Miele,A., Bystricky,K. and Dekker,J. (2009) Yeast silent mating type loci form heterochromatic clusters through silencer protein-dependent long-range interactions. *PLoS Genet.*, **5**, e1000478.